# Local nonlinear rf forces in inhomogeneous magnetized plasmas

Jiale Chen and Zhe Gao

Citation: Physics of Plasmas **21**, 062506 (2014); doi: 10.1063/1.4882864
View online: http://dx.doi.org/10.1063/1.4882864
View Table of Contents: http://scitation.aip.org/content/aip/journal/pop/21/6?ver=pdfcov
Published by the AIP Publishing



# Local nonlinear rf forces in inhomogeneous magnetized plasmas

Jiale Chen[1,a)] and Zhe Gao[2]
[1]Institute of Plasma Physics, Chinese Academy of Sciences, Hefei 230031, China
[2]Department of Engineering Physics, Tsinghua University, Beijing 100084, China

(Received 16 January 2014; accepted 30 May 2014; published online 11 June 2014)

The local nonlinear forces induced by radio frequency (rf) waves are derived in inhomogeneous magnetized plasmas, where the inhomogeneity exists in the rf fields, in the static magnetic field as well as in the equilibrium density and temperature. The local parallel force is completely resonant, but a novel component dependent on those inhomogeneities is obtained as the result of the inhomogeneous transport of parallel resonant-absorbed momentum by the nonlinear perpendicular drift flux. In the local poloidal force, the component induced by the inhomogeneity of rf power absorption is also confirmed and it can be recognized as the residual effect from the incomplete cancellation between the rate of the diamagnetic poloidal momentum gain and the Lorentz force due to the radial diffusion-like flux. The compact expression for radial force is also obtained for the first time, whose nonresonant component is expressed as the sum of the ponderomotive force on particles and the gradients of the nonresonant perpendicular pressure and of the nonresonant momentum flux due to the finite temperature effect. Numerical calculations in a 1-D slab model show that the resonant component dependent on the inhomogeneities may be significant when the ion absorption dominates the resonant wave-particle interaction. A quantitative estimation shows that the novel component in the parallel force is important to understand the experiments of the ion-cyclotron-frequency mode-conversion flow drive. © *2014 AIP Publishing LLC*. [http://dx.doi.org/10.1063/1.4882864]

## I. INTRODUCTION

Plasma current and flow can benefit the confinement and the stability of magnetized plasma in tokamak.[1–3] The use of radio frequency (rf) power to drive plasma current and/or flow is therefore of general interest. In the last decade, there was a rapid growth of the experiment discoveries about the rf-driven flows[4–10] besides the intrinsic flow affected by rf heating and current drive.[11–18] Although there is no widely accepted theory for rf-driven flow experiments, previous analyses showed that the wave momentum deposition and the momentum redistribution induced by rf waves might play an important role in the magnitude and profile of the flows driven by ion cyclotron range of frequency (ICRF) waves via mode conversion (MC)[5,8,19] and lower hybrid waves (LHW).[20,21] Therefore, a complete analysis of rf-induced *local* forces including these effects is required in order to establish a more credible theory to understand the experiments and to improve the precision of rf-driven flow and current profiles.

There are three basic mechanisms by which an rf wave exerts local forces on bulk plasma or selected particles.[22] First, the resonant wave-particle interaction can produce a dissipative force, by which the wave deposits the momentum on resonant particles in analogy with the well-known process of photon absorption; therefore, we may call it direct drive force (DDF) or fundamental dissipative force. Second, the inevitable inhomogeneity of rf fields exerts the well-known nonresonant ponderomotive force (RPF) in the direction of the inhomogeneity. Third, the inhomogeneity of resonant wave-particle interaction can redistribute the momentum of resonant particles and then induce a shear force. This force is proportional to the gradient of rf fields but perpendicular to the direction of the inhomogeneity; therefore, may be called as RPF[23] or resonant momentum redistribution force.[22]

Among the above three mechanisms, of particular interest is the component of RPF, since there is a steep gradient of rf fields in the direction perpendicular to the flux surface in a toroidal confinement equipment, which may play a key role in driving shear flows in both the poloidal and toroidal direction. The theoretical study of this component was started with the pioneering work on shear flows driven by the poloidal rf force.[24,25] However, the local ponderomotive effect in the flux surface was not correctly formulated until the kinetic stress was completely calculated in the second-order rf kinetic theory developed by Berry, Jaeger, and Batchelor.[26,27] A local resonant momentum redistribution force in the poloidal direction was then correctly recognized in Ref. 28. The perpendicular ponderomotive effect (including the off-diagonal stress) was also obtained from the guiding-center formulation of nonlinear rf kinetic theory by Myra, Berry, D'Ippolito, and Jaeger (MBDJ).[29] Besides the research on the perpendicular force, there are also a number of kinetic theoretical works on the toroidal force, or the parallel force in a slab model.[30–32] Using the complete kinetic stress calculated from the second-order rf kinetic theory, a local parallel force was reached to clear up the long-standing dispute on the toroidal current drive by nonresonant forces (see Ref. 33 and references therein). Recently, the complete parallel force due to the perpendicular inhomogeneity of rf fields was formulated and then discussed in the picture of a single particle, a fluid element, and a kinetic plasma, respectively.[23]

a)Electronic mail: chen@ipp.ac.cn

 

In this paper, the calculation of rf forces is extended to the cases with inhomogeneous equilibrium magnetic field, density, and temperature. In the previous derivations of parallel and poloidal RPFs, an inhomogeneous rf fields is considered but the inhomogeneities of the equilibrium parameters are neglected. Although the gradients of these equilibrium parameters are usually small, they might induce large gradients of other quantities in the local resonance zone. For example, it is well known that the small gradient of magnetic field is indispensable for the highly localized power deposition for cyclotron resonance. For another example, the gradient of the parallel resonant velocity $v_l^{(\mathrm{res})} \equiv (\omega - l\Omega)/k_{//}$ may contribute as greatly as that of rf fields to the parallel RPF given in Eq. (4). For cyclotron resonance ($l \neq 0$), the gradient is mainly due to the inhomogeneity of magnetic field $\mathbf{B}_0$, but is usually much larger than the gradient of $\mathbf{B}_0$, i.e.,

$$\left|\frac{\nabla_\perp v_l^{(\mathrm{res})}}{v_T}\right| \approx \left|\frac{l}{L_B k_{//}\rho}\right| \gg \frac{1}{L_B}, \tag{1}$$

where $L_B$ represents the characteristic length of $\mathbf{B}_0$ and $\rho$ represents the gyro radius. This gradient of $v_l^{(\mathrm{res})}$ was neglected in previous works. Another conclusion is confirmed in the present paper that there is no nonresonant parallel force even if the equilibrium and the rf field are both perpendicular inhomogeneous.

The physic pictures of the rf forces are discussed in the present paper. Especially, the diamagnetic flow and the diffusion-like flow due to the gyro-harmonic heating are found to be concomitant to the poloidal RPF and might be more important than it in future analysis for the rf-driven flow.

The paper is organized as follow. In Sec. II, the compact expressions of rf forces for quick references are presented as well as the discussion of mechanisms involved. In Sec. III, an extension of the guiding-center formulation is described and it is used to derive the rf forces given in Sec. II. The extension mainly modifies the manipulation of $v_l^{(\mathrm{res})}$ and then influences the rf forces. In Sec. III C, the derivation from guiding-center formulation to the parallel force is given, which was not considered in any previous research. Numerical calculations are given in Sec. IV to estimate the RPFs compared to the DDFs. A discussion on the role of the parallel RPF in ICRF MC flow drive is given in Sec. V. This is followed by a summary in Sec. VI. The detailed derivations for the energy absorption and the forces are presented in Appendixes A and B, respectively. In Appendix C, the general wave-momentum conservation equation (MCE) is given to be compared against the nonresonant ponderomotive force.

## II. LOCAL NONLINEAR RF FORCES AND COLLISIONLESS FLUXES

This section provides a quick reference about the expressions of the local nonlinear rf forces from the guiding-center formulation of rf-kinetic theory. Perpendicular to the static magnetic field are the inhomogeneities of the rf fields, of the static magnetic field, and of the equilibrium density and temperature. However, the magnetic shear is neglected for simplicity. The rf forces are calculated to the first order in $\rho/L_\perp$, where $L_\perp$ represents the shortest characteristic length of the inhomogeneities and $\rho$ is the gyroradius.

### A. Expressions of rf forces

The whole nonlinear local force $\mathbf{F}_2$ consists of two parts as

$$\mathbf{F}_2 = \mathbf{F}_\mathbf{k} + \mathbf{F}_\nabla, \tag{2}$$

where $\mathbf{F}_\mathbf{k}$ is the DDF and $\mathbf{F}_\nabla$ is the so-called *ponderomotive force* with explicit spatial dependence. The DDF is resonant as

$$\mathbf{F}_\mathbf{k} = \frac{1}{2}\mathrm{Re}\sum_{k,k'} \mathrm{e}^{i(\mathbf{k}'-\mathbf{k})\cdot\mathbf{r}} \frac{\mathbf{k}+\mathbf{k}'}{2\omega} \sum_l W_l(\mathbf{k},\mathbf{k}'), \tag{3}$$

where $W_l(\mathbf{k},\mathbf{k}') \equiv \mathbf{E}_k^* \cdot \mathbf{W}_l^{(\mathrm{ext})}(\mathbf{k},\mathbf{k}') \cdot \mathbf{E}_{k'}$ represents the energy absorption due to the $l$th cyclotron resonance[34] and $\mathbf{W}_l^{(\mathrm{ext})}(\mathbf{k},\mathbf{k}')$ is the extended W matrix given in Eq. (A9).

The parallel (to the static magnetic field $\mathbf{B}_0$) component of $\mathbf{F}_\nabla$ is resonant (and is thus the parallel RPF) as

$$\mathbf{b}\cdot\mathbf{F}_\nabla = -\frac{1}{2}\mathrm{Re}\nabla_\perp \cdot \sum_{k,k'} \mathrm{e}^{i(\mathbf{k}'-\mathbf{k})\cdot\mathbf{r}} \times \sum_l \frac{(\omega - l\Omega)\mathbf{k}\times\mathbf{b}}{\omega\Omega k_{//}} W_l(\mathbf{k},\mathbf{k}'), \tag{4}$$

where $(\omega - l\Omega)/k_{//}$ is just the parallel resonant velocity $v_l^{(\mathrm{res})}$ and $\mathbf{b} \equiv \mathbf{B}_0/|B_0|$. The perpendicular component is

$$(\mathbf{F}_\nabla)_\perp = \frac{1}{2}\mathrm{Re}\mathbf{b}\times\nabla_\perp \sum_{k,k'} \mathrm{e}^{i(\mathbf{k}'-\mathbf{k})\cdot\mathbf{r}} \sum_l \frac{l}{2\omega} W_l(\mathbf{k},\mathbf{k}') - \frac{1}{2}\mathrm{Re}\nabla_\perp \sum_{k,k'} \mathrm{e}^{i(\mathbf{k}'-\mathbf{k})\cdot\mathbf{r}} t \sum_l \frac{l\Omega}{\omega} W_l(\mathbf{k},\mathbf{k}') + \mathbf{F}_{\mathrm{nr}}. \tag{5}$$

When the inhomogeneities exist only in the radial direction (in tokamaks), the first term at RHS of Eq. (5) is the (resonant) poloidal force (i.e., the poloidal RPF) and the other terms constitute the radial force. The third term at RHS of Eq. (5) is the *only* nonresonant component in $\mathbf{F}_2$, which can be expressed as

$$\mathbf{F}_{nr} = -\frac{1}{2}\mathrm{Re}\sum_{k,k'} \mathrm{e}^{i(\mathbf{k}'-\mathbf{k})\cdot\mathbf{r}} \sum_l \frac{(\mathbf{k}'-\mathbf{k})}{2\omega} W_l(\mathbf{k},\mathbf{k}') - \frac{1}{2}\mathrm{Re}\nabla_\perp \sum_{k,k'} \mathrm{e}^{i(\mathbf{k}'-\mathbf{k})\cdot\mathbf{r}} \sum_l \frac{il\Omega}{2\omega}\frac{\partial W_l(\mathbf{k},\mathbf{k}')}{\partial\omega} - \frac{1}{2}\mathrm{Re}\nabla_\perp \sum_{k,k'} \mathrm{e}^{i(\mathbf{k}'-\mathbf{k})\cdot\mathbf{r}} \sum_l \frac{i\mathbf{k}_\perp}{2\omega}\cdot\frac{\partial W_l(\mathbf{k},\mathbf{k}')}{\partial\mathbf{k}_\perp}, \tag{6}$$

and it reduces to the conventional fluid ponderomotive force in the cold plasma limit.[35]

The expression forms of RPFs in Eqs. (4) and (5) are indeed the same as those in the homogeneous medium limit

which were obtained by directly calculating the moments of the 2nd order velocity distribution function $f_2$ (see Refs. 23 and 28 for the poloidal and parallel components, respectively). The complete expression of the nonresonant component even in the homogeneous limit has not been published elsewhere, but it is also consistent with the result by directly calculating the moments of $f_2$.[36] The mechanism of the ponderomotive force $\mathbf{F}_\nabla$ will be elaborated in the following subsections.

### B. Mechanisms of the parallel RPF

The parallel and poloidal components of $\mathbf{F}_\nabla$ are almost the same as the results in the homogeneous equilibrium[23,28] except that the W matrix and the gyro-frequency $\Omega$ here are space dependent. As for the mechanism, both these two components do not appear in the force in the single-particle picture, but result from the momentum transport through a fluid element. In contrast to the force on a single particle, the force on a Eulerian fluid element includes the components due to the stress and polarization but exclude that due to the displacement of a particle. Hence, the RPFs can still be obtained based on the analysis of the particle motion only if these differences were properly treated. More discussion using this particle-fluid approach has been given in Ref. 23. We directly describe the mechanism of every component of $\mathbf{F}_\nabla$ as below.

The $\mathbf{k}\times\mathbf{b}W_l/(\omega\Omega m)$ in Eq. (4) for parallel RPF is indeed the resonant-particle drift to balance the resonant wave-momentum absorption (proportion to $\mathbf{k}_\perp/\omega$). This drift is a second-order (in $\mathbf{E}_1$) response and transports the zero-order (in $\mathbf{E}_1$) parallel momentum of the "resonant particles," $mv_l^{(res)}$. The inhomogeneous transport of parallel momentum generates the parallel component of $\mathbf{F}_\nabla$ as a distributed parallel force without providing an integrated force over a plasma volume. In the derivation using the particle-fluid approach, the parallel component comes from the term $-\nabla\cdot(m\mathbf{v}_2 v_{0,//})$, which is directly recognized as the momentum transport by the resonant drift as $v_{0,//}=v_l^{(\mathrm{res})}$.[23]

The result in the present paper emphasizes that the gradient of $mv_l^{(res)}$ may contribute as greatly as that of rf fields to $-\nabla\cdot(m\mathbf{v}_2 v_{0,//})$ for cyclotron resonance, which can be perceived as follow. For cyclotron resonance ($l\neq 0$), the gradient of energy absorption in Eq. (4) can be estimated as

$$\left|\frac{\nabla W_l}{W_l}\right|\sim\left|\frac{\nabla\zeta_l}{\zeta_l}\right|\sim\frac{1}{\zeta_l}\left|\frac{\nabla_\perp v_l^{(\mathrm{res})}}{v_T}\right|, \tag{7}$$

where Eq. (1) has been used and $\zeta_l\equiv(\omega-l\Omega)/(k_{//}v_T)$ is the crucial argument for evaluating the plasma dispersion function $Z_l(\zeta_l)$.

### C. Mechanisms of the poloidal RPF

The poloidal RPF in Eq. (5) is also a distributed force and has been analyzed several times since Jaeger *et al.* obtained the compact expression in 2000.[22,28,37] However, its physics might be clearer from the following analysis of the collisionless perpendicular momentum balance equation (MBE).

For simplicity, the system (including the rf waves) here is assumed to be homogeneous along the symmetry direction y and z, where x, y, and z refer to the radial, poloidal, and toroidal coordinates. The perpendicular flux $(n\mathbf{V}_\perp)_2$ contains a diffusion-like flux along x-direction. The diffusion-like flux is due to the inhomogeneous expanding of the gyroradius and can be perceived by using the particle-fluid approach as follow. The radial flux in a Eulerian element is related to the quantities of a single particle (or in a Lagrangian element) as

$$(nv)_{\mathrm{Eu},2x}=n_0v_{2x}-n_0\nabla\cdot\langle\mathbf{r}_1v_{1x}\rangle_t+v_{0x}\langle n_2-\mathbf{r}_1\cdot\nabla n_1\rangle_t, \tag{8}$$

where the numbers in subscripts represent the order in $\mathbf{E}_1$, $\langle\rangle_t$ represents the averaging over the fast varying scale and the linearized continuity equation is used. Noting $-n_0\nabla\cdot\langle\mathbf{r}_1v_{1x}\rangle_t=-(n_0/2)\partial_x\mathrm{d}_t\langle x_1^2\rangle_t$, neglecting the finite gyroradius effect (i.e., $v_{0\perp}=0$) and assuming the linear perpendicular perturbation is isotropy (i.e., $\langle x_1^2\rangle_t=\langle y_1^2\rangle_t=\langle\rho_1^2\rangle_t/2$), we obtain $-n_0\nabla\cdot\langle\mathbf{r}_1v_{1x}\rangle_t=-(n_0/4)\partial_x\mathrm{d}_t\langle\rho_1^2\rangle_t$ which produces the diffusion-like flux.

From the second-order kinetic theory,[38] the complete expression of collisionless perpendicular flux $(n\mathbf{V}_\perp)_2$ is

$$\begin{aligned}(n\mathbf{V}_\perp)_2=&\frac{1}{qB}\mathbf{F}_\mathbf{k}\times\mathbf{b}+\frac{1}{qB}\mathbf{F}_{\mathrm{nr}}\times\mathbf{b}\\&+\hat{\mathbf{e}}_y\frac{1}{2qB}\mathrm{Re}\frac{\partial}{\partial x}\sum_{k,k'}\mathrm{e}^{i(\mathbf{k}'-\mathbf{k})\cdot\mathbf{r}}t\sum_l\frac{l\Omega}{\omega}W_l(\mathbf{k},\mathbf{k}')\\&-\hat{\mathbf{e}}_x\frac{1}{2qB}\mathrm{Re}\frac{\partial}{\partial x}\sum_{k,k'}\mathrm{e}^{i(\mathbf{k}'-\mathbf{k})\cdot\mathbf{r}}\sum_l\frac{l}{2\omega}W_l(\mathbf{k},\mathbf{k}').\end{aligned} \tag{9}$$

The first two terms at the RHS of Eq. (9) are the drifts due to DDF and the nonresonant ponderomotive force, respectively; the third term is the diamagnetic drift due to inhomogeneous gyro-harmonic heating; the last term is the diffusion-like flux.

Now, the radial and poloidal MBEs can be discussed with the use of $(n\mathbf{V}_\perp)_2$ in Eq. (9). The time derivative of $(n\mathbf{V}_\perp)_2$ is zero except its poloidal component $\partial(nV_y)_2/\partial t$ due to the diamagnetic drift, so the radial and poloidal components of MBE become, respectively

$$-qB_0(nV_y)_2=F_{2,x}, \tag{10}$$

$$m\frac{\partial}{\partial t}(nV_y)_2+qB_0(nV_x)_2=F_{2,y}. \tag{11}$$

For the case of $k_y=0$, $(\mathbf{F}_\mathbf{k})_y=0$ and the ratio of the terms in Eq. (11) is

$$m\frac{\partial}{\partial t}(nV_y)_2:qB_0(nV_x)_2:F_{2,y}=2:-1:1. \tag{12}$$

The causal relations between the collisionless flux and the perpendicular forces are different in consideration of the MBEs. From Eq. (10), the poloidal flux can be viewed as the drift caused by the radial rf force. In contrast, the poloidal RPF can be viewed as the residual effect due to the incomplete cancellation between the rate of the diamagnetic poloidal momentum gain and the Lorentz force due to the radial

diffusion-like flux in consideration of Eqs. (11) and (12). Thus, the diamagnetic drift and the diffusion-like flux should be considered prior to the poloidal RPF as the direct response to the rf heating in the analysis of the rf-driven flow.

### D. Mechanisms of other components

The radial component of rf force in Eq. (5) includes the radial DDF, a secular ($\propto t$) pressure gradient due to inhomogeneous gyro-harmonic heating, and a nonresonant ponderomotive force $\mathbf{F}_{nr}$ given in Eq. (6). The first term of $\mathbf{F}_{nr}$ just represents the ponderomotive force in the single particle picture, the second term represents the gradient of nonresonant perpendicular pressure, and the last term is due to some finite temperature effect which becomes zero in the cold plasma limit. Since the kinetic stress is neglected in the derivation of the wave-momentum conservation equation,[39] $\mathbf{F}_{nr}$ here cannot be described just as "photon reflection." This may contrast to some conventional but unproved ideas on the relation between the nonresonant/reactive ponderomotive force and the analogy of photon reflection.[31,40] This also indicates that the ponderomotive effect cannot be obtained just based on the wave kinetic equation. More details about the general wave-momentum equation are summarized in Appendix C.

The inhomogeneities bring about some first-order (in $\rho/L_\perp$) corrections in $\mathbf{F}_\mathbf{k}$ as well, but these corrections, in contrast to the RPFs, can contribute to the integrated force. They may come from the additional resonant interaction corresponding to the mixture of different electric field components without changing the basic physics of resonant momentum absorption.[23]

## III. EXTENDED GUINDING-CENTER FORMULATION FOR RF FORCES

In general, the nonlinear rf forces require the velocity distribution function to the second order in the wave amplitude, i.e., $f(\mathbf{v}) \approx f_0 + f_1 + \langle f_2 \rangle_t$. The distribution function $f$ is determined by the Vlasov equation

$$f(\mathbf{v}) \approx f_0 + f_1 + \langle f_2 \rangle_t, \tag{13}$$

where $\mathbf{a} \equiv (q/m)(\mathbf{E}_1 + \mathbf{v} \times \mathbf{B}_1)$, $\mathbf{E}_1$ and $\mathbf{B}_1$ are the applied rf fields. Since only the slowly varying part of $f_2$ is needed for the calculation of rf forces, the notation $\langle \rangle_t$ for the time average on nonlinear quantities will be suppressed where no confusion arises, e.g., $f_2 \equiv \langle f_2 \rangle_t$. The following abbreviation will frequently be used:

$$\langle A_1 B_1 \rangle_t = \frac{1}{2} \mathrm{Re} \sum_{k,k'} e^{i(\mathbf{k}'-\mathbf{k})\cdot\mathbf{r}} A_k^* B_{k'}. \tag{14}$$

In this work, the rf forces and the energy absorption are calculated to the first order in $f_2 \equiv \langle f_2 \rangle_t$, so quantities acted on by the gradient operator $\nabla$ are required only to the zero order.

There are three kinetic methods to derive the rf forces. The second-order rf kinetic theory developed by Berry, Jaeger, and Batchelor requires the explicit solution of $f_2$ and manipulations on triple products of Bessel functions to obtain the rf forces.[27] It is much more tedious to extend this method to consider the inhomogeneous magnetic field. The particle-fluid approach previously used by us requires the solution of particle motion equations.[23] Although this method is convenient to reveal the mechanisms, it is also tedious to be applied here. The guiding-center formulation developed by MBDJ can obtain the forces without the explicit expression of $f_2$, and thus is convenient to be extended to consider the inhomogeneities of equilibrium parameters although it was developed originally under the assumption of homogeneous equilibrium.[29] Therefore, the following derivation will be based on the extension of guiding-center formulation.

### A. Manipulation of energy absorption

The most significant modification due to the inhomogeneities of equilibrium parameters is on the resonant energy absorption, which should be separated from $\langle \mathbf{J}_1 \cdot \mathbf{E}_1 \rangle_t$.

For further derivation, we assume the static magnetic field as $\nabla \mathbf{B}_0 = (\nabla_\perp B_0)\mathbf{b}$ (i.e., retaining the inhomogeneity of magnetic-field amplitude but neglecting the magnetic shear and the magnetic curvature). For perpendicular inhomogeneous plasma, the equilibrium distribution function $f_0$ is not a Maxwellian with zero mean velocity. Assuming the gradients of density and temperature are in the same direction $\hat{\mathbf{e}}_{nT}$, we take $f_0$ as

$$f_0 = f_M \left[ 1 + \mathbf{R} \cdot \hat{\mathbf{e}}_{nT} \left( \varepsilon_n + \varepsilon_T \frac{v^2}{v_T^2} \right) \right], \tag{15}$$

where $f_M$ is the homogeneous Maxwellian, $v_T^2 \equiv 2T/m$, $\nabla \ln T = \varepsilon_T \hat{\mathbf{e}}_{nT}$, and $\nabla \ln n = (\varepsilon_n + 3\varepsilon_T/2)\hat{\mathbf{e}}_{nT}$.

We first solve the linearized Vlasov equation in the guiding-center coordinate system for the calculation of $\mathbf{J}_1$, and then evaluate $\langle \mathbf{J}_1 \cdot \mathbf{E}_1 \rangle_t$ to the first order in $\rho/L_\perp$ (more details are given in Appendix A). In the derivation, we adopt another assumption $k_{//} \gg 1/L_B$, which indicates that the Doppler broadening dominates over the broadening due to the gradient of magnetic field for the cyclotron resonance.[41,42] Although there are some cases of practical interest beyond this assumption, it is valid for the numerical examples given in the present article. The final expression for $\langle \mathbf{J}_1 \cdot \mathbf{E}_1 \rangle_t$ is

$$\langle \mathbf{J}_1 \cdot \mathbf{E}_1 \rangle_t = S - \nabla \cdot \mathbf{Q}, \tag{16}$$

where the energy absorption rate $S$ is

$$\begin{aligned} S = -\frac{q^2}{2\Omega T} \mathrm{Re} \int d^3\mathbf{v} K_\nabla f_M \sum_{k,k'} e^{i(\mathbf{k}'-\mathbf{k})\cdot\mathbf{r}} (\mathbf{E}_k^* \cdot \mathbf{v}) \\ \times e^{iH(\mathbf{k},\mathbf{r},\mathbf{v})} \int_{-\infty}^{\phi} d\phi' e^{-iH(\mathbf{k}',\mathbf{r},\mathbf{v})} (\mathbf{v} \cdot \mathbf{E}_{k'}), \end{aligned} \tag{17}$$

and the energy flow $\mathbf{Q}$ is

$$\mathbf{Q} = \frac{m}{2} \mathrm{Re} \sum_{k,k'} e^{i(\mathbf{k}'-\mathbf{k})\cdot\mathbf{r}} \int d^3\mathbf{v} \boldsymbol{\rho} (\mathbf{v} \cdot \mathbf{a}_k^*) f_{k'}. \tag{18}$$

By selecting $f_M$ as the zero-order (in $\rho/L_\perp$) distribution function at $\mathbf{r}$, the inhomogeneity factor $K_\nabla$ in Eq. (17) is

$$K_\nabla(\mathbf{r},\mathbf{v}) = 1 + \frac{1}{2\Omega\omega}(\mathbf{k}\cdot\mathbf{b}\times\mathbf{e}_{nT})\left(\varepsilon_n {v_T}^2 + \varepsilon_T v^2\right). \quad (19)$$

The integration of gyro-angles in Eq. (17) is further evaluated in Subsection 2 of Appendix to yield a W matrix, which is similar to that in Ref. 29 but includes the contribution from inhomogeneities.

The expressions about $\langle \mathbf{J}_1\cdot\mathbf{E}_1\rangle_t$ given by Eqs. (16)–(19) are the main results of our extension on the guiding-center formulation. Neglecting the spatial dependence of $\Omega(x)$ and taking $K_\nabla(\mathbf{r},\mathbf{v})\approx 1$, the expressions reduce to those given in the original guiding-center formulation, i.e., Eqs. (A10), (A20)–(A22) in Ref. 29. However, the spatial dependence of $\Omega(x)$ is significant for the evaluation of the gradients of energy absorption and rf forces due to the cyclotron-harmonic resonance. It should be noted that the gradients of the equilibrium parameters (in the energy absorption) were also retained in Ref. 28 by appealing to the argument of the global momentum conservation, and its contribution is usually larger than that from the gradient of the rf fields.[43]

It is critical to separate the pure resonant component $S$ from $\langle \mathbf{J}_1\cdot\mathbf{E}_1\rangle_t$ not only for distinguish the resonant energy absorption from the energy flux but also for recognizing the mechanism of the rf forces. The $S$ given in Eq. (17) just represents the resonant energy absorption since it is a symmetric bilinear form on $\mathbf{E}_k$ (or $\mathbf{E}_{k'}$). Therefore, $S(\mathbf{k}+\mathbf{k}')/2\omega$ is just the DDF corresponding to the resonant momentum absorption.

### B. The guiding-center formulation for rf forces

In this subsection and Appendix B, we briefly summarize the derivation of rf forces in Ref. 29 including our extension in Sec. III A. The rf force on each plasma species is the sum of the nonlinear electromagnetic (EM) force and the gradient of the kinetic stress, i.e., $\mathbf{F}_2 \equiv \mathbf{F}_L - \nabla\cdot\mathbf{\Pi}_2$. The kinetic stress can be separated as $\mathbf{\Pi}_2 = \mathbf{\Pi}_\phi + \mathbf{\Pi}_{\mathrm{CGL}}$, where

$$\mathbf{\Pi}_\phi = m\int \mathrm{d}^3\mathbf{v}\left(\mathbf{vv} - \langle\mathbf{vv}\rangle_\phi\right)\tilde{f}_2, \quad (20)$$

$$\mathbf{\Pi}_{\mathrm{CGL}} \equiv m\int \mathrm{d}^3\mathbf{v}\langle\mathbf{vv}\rangle_\phi\langle f_2\rangle_\phi, \quad (21)$$

$\langle f_2\rangle_\phi$ and $\tilde{f}_2$ are, respectively, the gyrophase independent part and gyrophase dependent part of $f_2$. The detailed expressions of $\mathbf{\Pi}_\phi$ and $\mathbf{\Pi}_{\mathrm{CGL}}$ are given in Eqs. (B2) and (B8), respectively. The nonlinear EM force $\mathbf{F}_L \equiv \langle qn_1\mathbf{E}_1 + q(n\mathbf{V})_1\times\mathbf{B}_1\rangle_t$ can be rewritten as[29]

$$\mathbf{F}_L = \frac{1}{2}\mathrm{Re}[(\nabla\mathbf{E}^*)\cdot\mathbf{D}] - \nabla\cdot\mathbf{\Pi}_{\mathrm{DE}}, \quad (22)$$

where $\mathbf{\Pi}_{\mathrm{DE}} = \mathrm{Re}(\mathbf{DE}^*)/2$, $\mathbf{D}$ represents $\sum_{k'}(i\mathbf{J}_{k'}/\omega)\exp(i\mathbf{k}'\cdot\mathbf{r})$ and $\mathbf{E}^*$ represents $\sum_k \mathbf{E}_k{}^*\exp(-i\mathbf{k}\cdot\mathbf{r})$. Noting

$$(\nabla\mathbf{E}^*)\cdot\mathbf{D} = \sum_{k,k'} \mathrm{e}^{i(\mathbf{k}'-\mathbf{k})\cdot\mathbf{r}}\frac{\mathbf{k}}{\omega}\mathbf{E}_k^*\cdot\mathbf{J}_{k'}, \quad (23)$$

and using Eqs. (16)–(8) and (18) for the manipulation of $\mathbf{E}_k^*\cdot\mathbf{J}_{k'}$, we obtain

$$\frac{1}{2}\mathrm{Re}[(\nabla\mathbf{E}^*)\cdot\mathbf{D}] = \mathbf{F}_\mathbf{k} + \mathbf{F}_r - \nabla\cdot\mathbf{\Pi}_w, \quad (24)$$

$$\mathbf{F}_\mathbf{k} = \frac{1}{2}\mathrm{Re}\sum_{k,k'}\mathrm{e}^{i(\mathbf{k}'-\mathbf{k})\cdot\mathbf{r}}\frac{\mathbf{k}+\mathbf{k}'}{2\omega}\sum_l W_l(\mathbf{k},\mathbf{k}'), \quad (25)$$

$$\mathbf{F}_\mathrm{r} = -\frac{1}{2}\mathrm{Re}\sum_{k,k'}\mathrm{e}^{i(\mathbf{k}'-\mathbf{k})\cdot\mathbf{r}}\frac{(\mathbf{k}'-\mathbf{k})}{2\omega}\sum_l W_l(\mathbf{k},\mathbf{k}'), \quad (26)$$

$$\mathbf{\Pi}_w = \frac{m}{2}\mathrm{Re}\sum_{k,k'}\mathrm{e}^{i(\mathbf{k}'-\mathbf{k})\cdot\mathbf{r}}\int \mathrm{d}^3\mathbf{v} f_{k'}\rho\mathbf{v}\cdot\mathbf{a}_k^*\frac{\mathbf{k}}{\omega}. \quad (27)$$

Then, the total rf force is obtained as $\mathbf{F}_2 = \mathbf{F}_\mathbf{k} + \mathbf{F}_\nabla$, where

$$\mathbf{F}_\nabla = \mathbf{F}_\mathrm{r} - \nabla\cdot(\mathbf{\Pi}_w + \mathbf{\Pi}_{DE} + \mathbf{\Pi}_\phi) - \nabla\cdot\mathbf{\Pi}_{\mathrm{CGL}}. \quad (28)$$

$\mathbf{F}_\mathbf{k}$ in Eq. (25) is a symmetric bilinear form on $\mathbf{E}_k$ (or $\mathbf{E}_{k'}$) and thus only includes resonant terms. This conclusion on $\mathbf{F}_\mathbf{k}$ is the main result on rf forces from the extension of guiding-center formulation, since the calculation for $\mathbf{F}_\nabla$ needs only the zero-order modification [i.e., $K_\nabla\approx 1$ but retaining the spatial dependence of $\Omega(x)$].

In conclusion, the present article confirms the framework by MBDJ.[29] In their work, the perpendicular component of $\mathbf{F}_\nabla$ was considered. The correct poloidal RPF was obtained but the radial nonresonant force was wrong. Nevertheless, most of their derivation is still valid here and is summarized in Subsection 2 of Appendix B, where our modification is also pointed out (especially, there was a mistake in the Ref. 29 in the calculation for the nonresonant force). Since the parallel force was not considered in the original MBDJ's work, we will present the derivation for it in the following subsection.

### C. Parallel rf forces due to perpendicular gradients

Restricting the derivation to the case with only perpendicular gradients, we obtain from Eq. (28) the parallel force

$$F_{//} = \mathbf{F}_\mathbf{k}\cdot\mathbf{b} - \nabla_\perp\cdot(\mathbf{\Pi}_w + \mathbf{\Pi}_{\mathrm{DE}} + \mathbf{\Pi}_\phi)\cdot\mathbf{b}, \quad (29)$$

where $\mathbf{F}_\mathbf{k}\cdot\mathbf{b}$ is the parallel DDF and the remainder components will give the parallel RPF as follow. Combining Eqs. (27), (B1), and (B2) for the stress terms, we have

$$-\nabla_\perp\cdot(\mathbf{\Pi}_\phi + \mathbf{\Pi}_{\mathrm{DE}} + \mathbf{\Pi}_w)\cdot\mathbf{b} = -\nabla_\perp\cdot\left[\left\langle\frac{m}{\Omega}\int \mathrm{d}^3\mathbf{v}(\mathbf{a}_1\times\mathbf{b}v_{//})f_1\right\rangle_t - \frac{1}{2}\mathrm{Re}\sum_{k,k'}\mathrm{e}^{i(\mathbf{k}'-\mathbf{k})\cdot\mathbf{r}}\frac{in_0 q}{\omega B}\mathbf{b}\times\mathbf{E}_{k'}E_{k,//}^*\right], \quad (30)$$

where the second term in the square bracket was omitted in the original MBDJ work but it is necessary to cancel the non-resonant terms in the first term.

Substitute the lowest-order $f_{k'}$ from Eq. (A5) into Eq. (30) to obtain the same result we obtain the parallel RPF as

$$-\nabla_\perp \cdot (\mathbf{\Pi}_\phi + \mathbf{\Pi}_{\mathrm{DE}} + \mathbf{\Pi}_w) \cdot \mathbf{b} = -\frac{1}{2}\mathrm{Re}\nabla_\perp \cdot \sum_{k,k'} e^{i(\mathbf{k}'-\mathbf{k})\cdot\mathbf{r}} \sum_l \frac{v_l^{(\mathrm{res})}\mathbf{k}\times\mathbf{b}}{\omega\Omega} W_l(\mathbf{k},\mathbf{k}'). \quad (31)$$

Another derivation without using the solution of $f_{k'}$ is given in Subsection 3 of Appendix B.

## IV. NUMERICAL COMPARISON BETWEEN DDF AND RPF

In order to estimate the magnitude of the RPF compared to the DDF, we use a perpendicular stratified, one-dimensional slab plasma model, where (x, y, z) might refer to the radial, poloidal, and toroidal coordinates in a tokamak, respectively.[27] Assuming that the scale length of power deposition is $L_{rf} \sim L_\perp$, the ratio of the parallel RPF to the parallel DDF is approximately $F_{RPF}/F_{DDF} \approx k_y\rho_T v_l^{(res)}/(k_z L_{rf} v_T)$. It implies that for nearly perpendicular propagating wave the effect of the RPF might be significant. Furthermore, $L_{rf}$ is expected to be small for the cyclotron damping (i.e., $l \neq 0$) and can be estimated as $L_{rf} \sim \zeta_l L_B k_z \rho_T / l$, where Eq. (7) has been used and $L_B$ is roughly the major radius $R_0$ in tokamaks. Then the ratio becomes $F_{RPF}/F_{DDF} \approx l k_y/(\zeta_l k_z^2 R_0)$, and thus shows a strong sensitivity on $k_z$. In the following numerical examples, it is thus expected that the ratio for ECRF is much smaller than that for ICRF, since $k_z$ is much larger in the former case. Similarly for the poloidal force, the ratio of RPF to the DDF becomes $F_{RPF}/F_{DDF} \approx l/(\zeta_l k_y \rho_T k_z L_B)$. It is also expected that the ratio for ECRF is much smaller than that for ICRF.

Now, we present numerical examples to estimate the RPFs in comparison against the DDFs. Neglecting the magnetic shear we consider a 1-D slab tokamak plasma with major radius $R_0 = 0.67$m, minor radius $a = 0.22$m, and the magnetic field on axis denoted as $B_0$. Fig. 1 presents the normalized parameter distributions with central density and temperature, respectively, as $n_{e,0} = 1.2 \times 10^{20}\mathrm{m}^{-3}$ and $T_{e,0} = T_{i,0} = 3.5$keV. Given the frequency and parallel wave-number for an rf wave, the perpendicular wave-number is calculated according to the local dispersion relation from the cold plasma model. The wave experiences the collisionless damping according to the energy absorption given in Eqs. (A8) and (A11). To explore the RPFs with a nonzero poloidal wavenumber $k_y$, we artificially set $k_y = k_x$ in the calculation for the forces. We also present the calculation of poloidal forces. It should be noted that the special cases for $k_y = 0$ in ICRF have been presented in Ref. 27, but without considering the DDFs as the comparison. All the forces are calculated with the condition that 1 MW power is absorbed by the corresponding particle species.

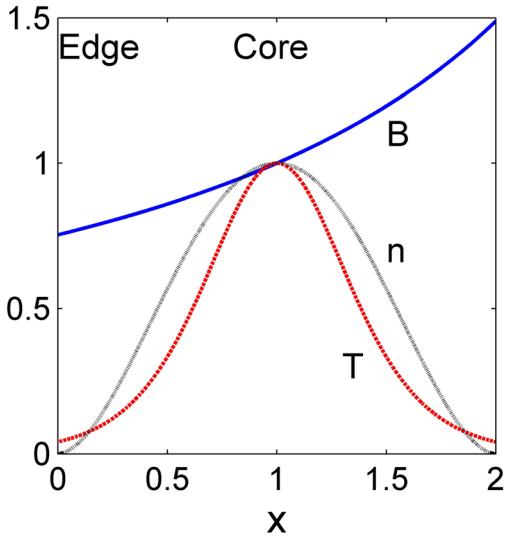


FIG. 1. Normalized equilibrium magnetic field, density and temperature profile for 1-D tokamak plasma with $R_0 = 0.67$m, $a = 0.22$m.

Fig. 2 shows the rf forces (actually, the force density in the unit $\mathrm{Nm}^{-3}$) on the minority hydrogen ions for a case of ICRFs. The frequency is chosen such that the second harmonic resonance of hydrogen dominates the power absorption of fast wave. The red solid line shows the DDF density $\mathbf{F}_\mathbf{k}$, and the black dotted line shows the RPF density $\mathbf{F}_\nabla$. The asterisk line shows the composite force density $\mathbf{F}_2 = \mathbf{F}_\mathbf{k} + \mathbf{F}_\nabla$. For both the parallel and poloidal forces, the RPFs dominate at the place with a large gradient of the DDF, and are able to change the direction of the composite force.

Fig. 3 shows the forces on electrons for a case of first harmonic resonance for O-mode electron cyclotron wave (ECRF). Since $k_z/L_B$ is much larger than the wavenumber ratio $k_\perp/k_z$ and $1/(k_y\rho_T)$, the RPFs are negligible to the total forces both in the toroidal and poloidal direction.

Fig. 4 shows the forces on electrons for a case of LHW. Although the lower hybrid wave propagates nearly perpendicularly, $k_\perp/k_z$ is not large enough to offset $\rho/L_{rf}$. The RPFs are negligible to the total forces. It should be noted that the parallel wavenumber $k_z$ (or refractive index $n_z$) is set large enough to make the wave damp greatly before propagating out of this 1-D slab model. It may be possible that the parallel RPF has a considerable effect if $k_y$ becomes large while $k_z$ stays small. However, the mechanisms causing the poloidal wavenumber varying are still controversial at present.[44–49]

From these examples, it is conjectured that the parallel PRF might be significant for the ion Bernstein wave (IBW). The IBW has a large perpendicular wave vector $k_\perp\rho_i \sim 1$ and a rather low parallel wave vector $ck_{//}/\omega \sim 1$. In fact, in the case of the mode-converted IBW, the parallel wave vector actually vanishes as it flips sign.[50] Then, one has $F_{RPF}/F_{DDF} \approx c^2/(\omega^2\rho_i R_0)$, which is much large in typical IBW experiments. Therefore, the RPF is expected to play a key role in the scheme of IBW flow drive.

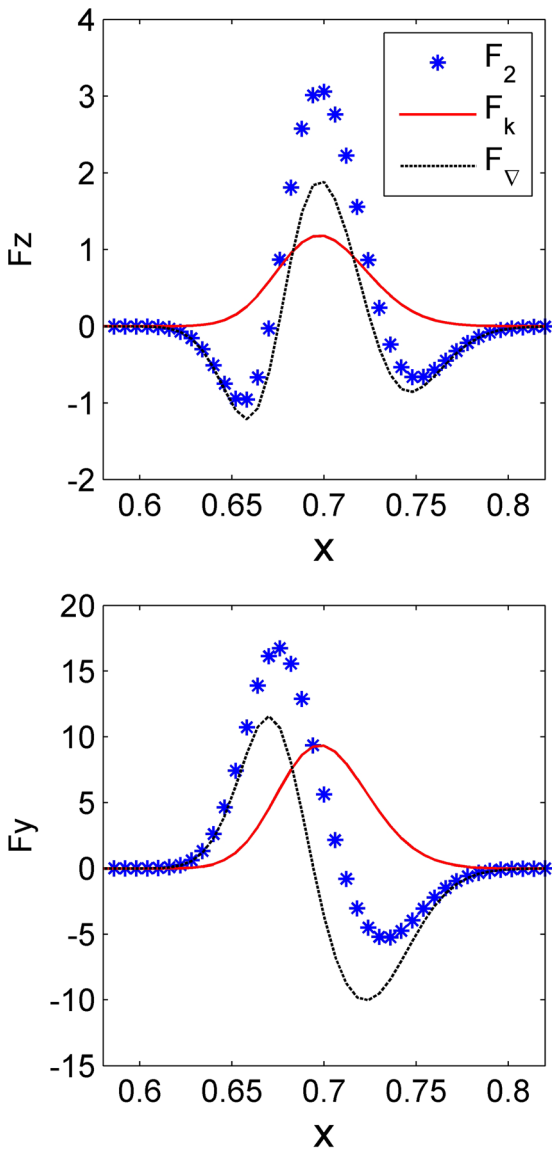


FIG. 2. The parallel forces (top) and poloidal forces (bottom) on the minority hydrogen ions when the second harmonic resonance on hydrogen dominates the power absorption of fast wave; $n_H/(n_H + n_D)$=0.1, $B_0 = 3.6$T, $f = 100$MHz, and $k_z = 10\text{m}^{-1}$; $\mathbf{F}_k$, $\mathbf{F}_\nabla$, $\mathbf{F}_2$ are the DDF, the RPF, and the composite force, respectively.

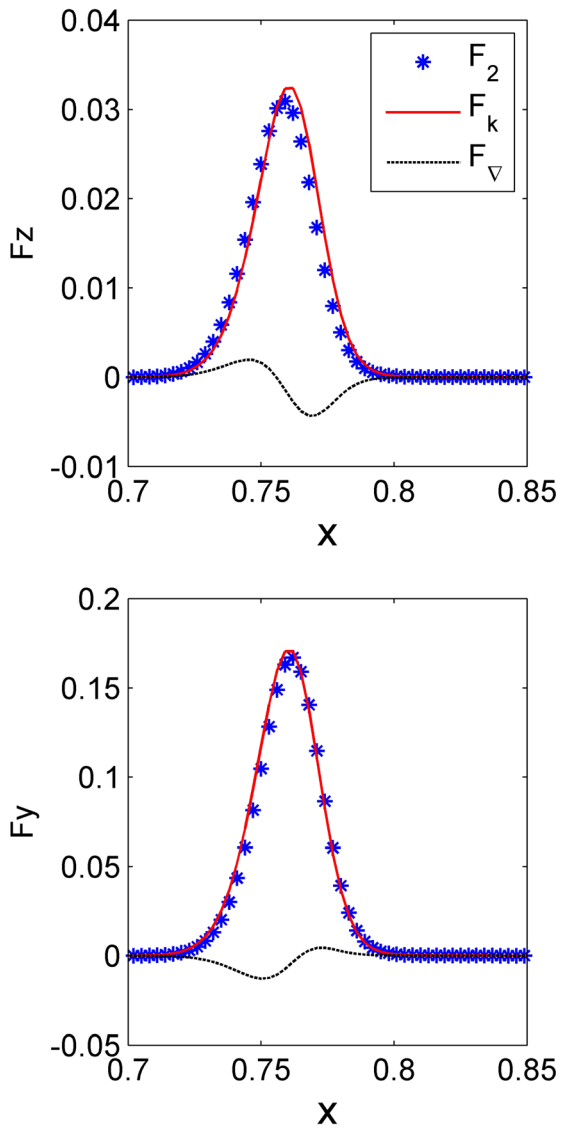


FIG. 3. The parallel forces (top) and poloidal forces (bottom) on the electrons for O-1 mode of electron cyclotron wave; $B_0 = 5.3$T, $f = 140$GHz, and the parallel refractive index $n_z = 0.1$; $\mathbf{F}_k$, $\mathbf{F}_\nabla$, $\mathbf{F}_2$ are the DDF, the RPF, and the composite force, respectively.

## V. DISCUSSION OF THE PARALLEL RPF IN ICRF MC FLOW DRIVE

For rf heating, the RPFs could dominate since the DDFs almost cancel due to the symmetric wave-vector spectrum. It is more subtle for the parallel RPF which is proportional to $\hat{\mathbf{e}}_\psi \cdot \mathbf{k} \times \mathbf{b}/k_{//}$, where $\hat{\mathbf{e}}_\psi$ denotes the unit vector perpendicular to the flux surface. Here, $k_{//} = k_\theta \hat{\mathbf{e}}_\theta \cdot \mathbf{b} + k_\phi \hat{\mathbf{e}}_\phi \cdot \mathbf{b}$, where $\hat{\mathbf{e}}_\theta$ and $\hat{\mathbf{e}}_\phi$ denote the unit vectors along the poloidal and toroidal direction, respectively. For the mode-converted ICW and IBW[19] $k_{//} \approx k_\theta \hat{\mathbf{e}}_\theta \cdot \mathbf{b} \gg k_\phi$, so $\hat{\mathbf{e}}_\psi \cdot \mathbf{k} \times \mathbf{b}/k_{//} \approx \hat{\mathbf{e}}_\theta \cdot \mathbf{b} \times \hat{\mathbf{e}}_\psi / \hat{\mathbf{e}}_\theta \cdot \mathbf{b}$ and the parallel RPF is independent to the symmetry of the $\mathbf{k}$ spectrum. In contrast, the parallel wave-vector satisfies $k_{//} \sim k_\theta \hat{\mathbf{e}}_\theta \cdot \mathbf{b} \sim k_\phi$ for the ICRF via minority heating (MH), and, therefore, the parallel RPF might be dependent on the $\mathbf{k}$ spectrum and greatly reduce if the spectrum at the resonance is highly symmetric. These features might account for the experimental observation that the rf-driven toroidal flow plays a significant role in ICRF via MC but not in ICRF via MH.[51]

In order to estimate the flow driven by the parallel RPF in ICRF via MC in Alcator C-Mod, we use the information about the power deposition from TORIC[52] simulation published in Ref. 51. For ICRF MC heating, the power deposition to the minority $^3$He ions is mainly through the MC ICW. The maximum of its profile after averaging over flux surface is $P_{\max} \sim 7.5\text{MW}/m^3$ at $r \sim 0.4a$ and its characteristic length for the *interior* region (specifically $0.1 < r/a < 0.4$) is about $0.3a$, where the small radius is $a = 0.22$ m. The ICW is about 4 cm on the high field side of the $^3$He fundamental resonance layer, which is at about $R \sim 70$ cm. The wave frequency is 50MHz, while the absolute values of the parallel and

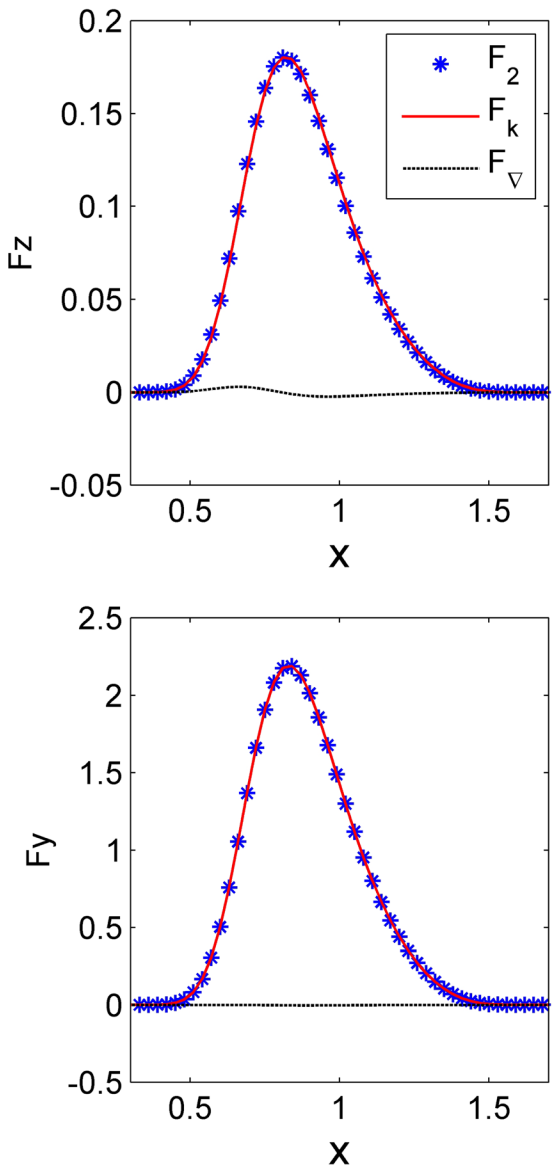


FIG. 4. The parallel forces (top) and poloidal forces (bottom) on the electrons for lower hybrid wave; $B_0 = 5.3\text{T}$, $f = 4.6\text{GHz}$, and the parallel refractive index $n_z = 5$; $\mathbf{F}_k$, $\mathbf{F}_\nabla$, $\mathbf{F}_2$ are the DDF, the RPF, and the composite force, respectively.

perpendicular wavenumbers are, respectively, $|k_{||}| \sim 45m^{-1}$ and $|\hat{\mathbf{e}}_\psi \cdot \mathbf{k} \times \mathbf{b}| \sim 500m^{-1}$. The parallel RPF from Eq. (4) is roughly $F_{RPF,||} \sim 0.23\text{N}/m^3$ along the concurrent direction in the interior region. For simplicity, one may ignore the details of toroidal momentum transport but consider that the rf-driven toroidal flow would relax in the toroidal momentum confinement time $\tau_\phi$ if the rf power is shut off. Neglecting the momentum flux through the boundary for simplicity, the zero dimensional toroidal angular momentum equation for the interior region is approximately[20]

$$\partial_t \langle R^2 \nabla\phi \cdot n_i m_i \mathbf{u}_i \rangle + \frac{1}{\tau_{\varsigma,i}} \langle R^2 \nabla\phi \cdot n_i m_i \mathbf{u}_i \rangle = \langle R^2 \nabla\phi \cdot \mathbf{F}^{\text{w}} \rangle, \tag{32}$$

where $\langle\rangle$ denotes the magnetic flux surface average and the toroidal momentum confinement time is $\tau_{\phi,i} \sim 80\text{ms}$. In the following discussion, we apply the steady state assumption $\partial_t = 0$. The electron density is $n_e \sim 1 \times 10^{20}\text{m}^{-3}$ and $n_{^3He}/n_e \sim 10\%$, so the effective mass density is $n_i m_i \sim 3.2 \times 10^{-7}\text{kg}/m^3$. The toroidal rf force is approximately $R\nabla\phi \cdot \mathbf{F}^{\text{w}} \sim F_{RPF,||}$ where the DDFs are neglected due to the symmetry of $\mathbf{k}$ spectrum and the poloidal RPF is neglected due to $B_\theta/B_\phi \ll 1$. With the above parameters, the change of toroidal velocity due to ICRF via MC in the interior region is $\sim 60\text{km}/s$ which roughly equals the difference between the MC and MH driven flows in the experiment.

Before concluding this session, we should point out that the parallel RPF is essentially an rf-induced stress which can transport the concurrent toroidal momentum inward across the broad MC ICW deposition region, and is independent to the gradient and the value of the toroidal velocity. Although the parallel RPF is dipole-like, the enhancement of toroidal momentum transport would change the global toroidal momentum like other stress (e.g., turbulent stress and collisional stress).

The above applications of the rf forces are nevertheless preliminary estimation. More calculations are ongoing including the direct calculation using a 2D RF code (like TORIC) to produce the rf forces and applying a more realistic transport model for toroidal momentum transport.[53]

## VI. SUMMARY

In this paper, we extend the guiding-center formulation developed by MBDJ to obtain the rf kinetic forces including the effect of perpendicular inhomogeneities in the rf fields, in the static magnetic field, and in the equilibrium plasma density and temperature. It is proved that the decomposition, $\langle \mathbf{J}_1 \cdot \mathbf{E}_1 \rangle_t = S - \nabla \cdot \mathbf{Q}$, is still valid and the local energy absorption is completely resonant if the resonance broadening is dominated by the Doppler broadening due to finite $k_{//}$.

The local parallel force is completely resonant, but it consists of two parts: one is the DDF (direct drive force, aka fundamental dissipative force) due to resonant parallel momentum absorption; the other is the RPF (resonant ponderomotive force, aka resonant momentum redistribution effect) due to the radial inhomogeneities of the poloidal momentum absorption and the resonant velocity, which is given in Eq. (4). The RPF is an actual nonlinear force in thermal plasmas, and originates from the inhomogeneous transport of parallel momentum of resonant particles by the nonlinear perpendicular drift flux. The poloidal RPF reported previously by Jaeger *et al.*[28] is confirmed again and re-understood as a residual effect due to the incomplete cancellation between the rate of the poloidal momentum gain and the Lorentz force due to the radial particle flux. The poloidal momentum gain is just the diamagnetic drift by the inhomogeneous perpendicular heating, and the radial particle flux is a diffusion-like flow due to the gyroradius expanding of "resonant particles." The radial force composes of the DDF, the secular resonant pressure gradient, and the nonresonant ponderomotive force. The nonresonant force is further expressed as the sum of the ponderomotive force on particles, the gradients of the

nonresonant pressure and of the nonresonant momentum flux due to finite temperature effect.

The numerical comparison in a slab rf model shows that the RPFs in both the parallel and poloidal directions are comparable to the DDFs when ion absorption dominates (e.g., in ICRF) but negligible when electron absorption dominates (e.g., in ECRF and LHW). For ICRF MC flow drive, the parallel RPF is independent to the symmetry of $\mathbf{k}$ spectrum and its significance is demonstrated by a preliminary quantitative estimation. More detail for the flows driven by rf forces will be explored in upcoming works.

## ACKNOWLEDGMENTS

This work was supported by NSFC, under Grant Nos. 11325524, 10990214, and 11261140327, MOST of China, under Contract Nos. 2013GB112001 and 2011GB105004, Tsinghua University Initiative Scientific Research Program and 221 Program.

## APPENDIX A: MANIPULATION FOR ENERGY ABSORPTION

### 1. The linearized velocity distribution function

The transformation from lab coordinates $(\mathbf{r}, \mathbf{v})$ to guiding center coordinates $(\mathbf{R}, \mathbf{V})$ is given by

$$\mathbf{r} = \mathbf{R} + \boldsymbol{\rho}(\mathbf{R}, \mathbf{V}); \quad \boldsymbol{\rho}(\mathbf{R}, \mathbf{V}) \equiv \frac{\mathbf{b}(\mathbf{R})}{\Omega(\mathbf{R})} \times \mathbf{V} \quad \mathbf{v} = \mathbf{V}. \tag{A1}$$

Thus, the transformed linearized Vlasov equation including the first-order inhomogeneity effect of $B_0$ is[54]

$$\left[\frac{\partial}{\partial t} + V_{//}\nabla_{//} - (\Omega + \boldsymbol{\rho}\cdot\nabla_{\mathbf{R}}\Omega)\partial_{\phi} + (\boldsymbol{\rho}\cdot\nabla_{\mathbf{R}}\Omega)\mathbf{V}_{\perp}\cdot\nabla_{\perp}\right] f_1 = -\mathbf{a}\cdot\nabla_V f_0 - \frac{1}{\Omega}\mathbf{a}\cdot\mathbf{b}\times\nabla_{\mathbf{R}} f_0. \tag{A2}$$

Using Eq. (15) and the Fourier representation of $\mathbf{a}$ as $\mathbf{a} = \sum_{k'} \mathbf{a}_{k'} e^{i\mathbf{k}'\cdot\mathbf{r}}$, the RHS of Eq. (A2) becomes

$$K_{nT}(\mathbf{k}', \mathbf{R}, \mathbf{v}) \equiv \frac{2f_M}{v_T^2}\mathbf{a}_{k'}\cdot\mathbf{v}\left[1 + \mathbf{R}\cdot\hat{\mathbf{e}}_{nT}\left(\varepsilon_n - \varepsilon_T + \varepsilon_T\frac{v^2}{v_T^2}\right)\right] - \frac{f_M}{\Omega}\mathbf{a}_{k'}\cdot\mathbf{b}\times\hat{\mathbf{e}}_{nT}\left(\varepsilon_n + \varepsilon_T\frac{v^2}{v_T^2}\right). \tag{A3}$$

We expand the linear response in the Fourier representation[55]

$$f_1 = \sum_{k'} f_{k'} e^{i\mathbf{k}'\cdot\mathbf{r}} = \sum_{k'} f_{k'} e^{i\mathbf{k}'\cdot\boldsymbol{\rho}} e^{i\mathbf{k}'\cdot\mathbf{R}}, \tag{A4}$$

and use the local approximation to keep the spatial dependence of equilibrium parameters which is supposed to vary much slowly than the linear rf-induced perturbation. Then, the solution of Eq. (A2) is obtained as

$$f_{k'} = -e^{iH(\mathbf{k}',\mathbf{R},\mathbf{V})}\int_{-\infty}^{\phi} d\phi'|_R e^{-iH(\mathbf{k}',\mathbf{R},\mathbf{V}')}\frac{K_{nT}(\mathbf{k}', \mathbf{R}, \mathbf{v}')}{\Omega(1 - \nabla\cdot\boldsymbol{\rho}')}, \tag{A5}$$

where $\boldsymbol{\rho}'\cdot\nabla\Omega = -\Omega\nabla\cdot\boldsymbol{\rho}'$ is used and the lowest-order $H$ is

$$H_0(\mathbf{k}', \mathbf{R}, \mathbf{V}) = -(\omega - k'_{//}v_{//})\frac{\varphi}{\Omega} - \boldsymbol{\rho}\cdot\mathbf{k}'_{\perp}. \tag{A6}$$

The higher-order terms in $H$ correspond to the cyclotron-harmonic coupling and hence can be neglected since $k_{\perp}\rho \ll L_B/\rho$ for most cases of practical interest. More discussion about this argument can be found in the work by Chen and Tsai about the gyrokinetic formulism for arbitrary frequency waves.[56]

### 2. The energy absorption

Making use of Eq. (A5) (to evaluate $\mathbf{J}_1$), we obtain $\langle\mathbf{J}_1\cdot\mathbf{E}_1\rangle_t$ to the first order in $\rho/L_{\perp}$ as

$$\langle\mathbf{J}_1\cdot\mathbf{E}_1\rangle_t = -\frac{1}{2}\mathrm{Re}\int d^3\mathbf{v}\sum_{k,k'} e^{i(\mathbf{k}'-\mathbf{k})\cdot\mathbf{R}} q(\mathbf{v}\cdot\mathbf{E}_k^*)e^{iH(\mathbf{k},\mathbf{R},\mathbf{v})} \times\int_{-\infty}^{\phi} d\phi'|_R e^{-iH(\mathbf{k}',\mathbf{R},\mathbf{v})}\frac{K_{nT}(\mathbf{k}', \mathbf{R}, \mathbf{v}')}{\Omega(1 - \nabla\cdot\boldsymbol{\rho}')}. \tag{A7}$$

Then, we expand the integrand at $\mathbf{R} = \mathbf{r}$ under the assumption that the parallel wave number is large enough, i.e., $k_{//} \gg 1/L_B$. Then, Eqs. (16)–(19) are obtained.

Completing the integration over the gyro-angle $\phi'$, the energy absorption rate in Eq. (17) becomes

$$S = \frac{1}{2}\mathrm{Re}\sum_{k,k'} e^{i(\mathbf{k}'-\mathbf{k})\cdot\mathbf{r}}\sum_{l} W_l(\mathbf{k}, \mathbf{k}'), \tag{A8}$$

where $W_l(\mathbf{k}, \mathbf{k}') \equiv \mathbf{E}_k{}^*\cdot\mathbf{W}_l^{(\mathrm{ext})}(\mathbf{k}, \mathbf{k}')\cdot\mathbf{E}_{k'}$,

$$\mathbf{W}_l^{(\mathrm{ext})}(\mathbf{k}, \mathbf{k}') \equiv \frac{q^2}{T}e^{il(\theta_{k'}-\theta_k)}\int d^3\mathbf{v}K_{\nabla}f_M\frac{i}{\bar{\omega}_l}\mathbf{H}_l(\mathbf{k})^*\mathbf{H}_l(\mathbf{k}'), \tag{A9}$$

$$\mathbf{H}_l(\mathbf{k}) \equiv \hat{\mathbf{k}}_{\perp}v_{\perp}\frac{l}{\lambda_k}\mathrm{J}_n(\lambda_k) + \mathbf{b}\times\hat{\mathbf{k}}_{\perp}v_{\perp}i\mathrm{J}'_l(\lambda_k) + v_z\mathrm{J}_l(\lambda_k)\hat{\mathbf{z}}, \tag{A10}$$

$\bar{\omega}_l \equiv \omega - l\Omega - k_{//}v_{//}$, $\lambda_k \equiv k_{\perp}v_{\perp}/\Omega$, $\hat{\mathbf{k}}_{\perp}$ is the unit vector along the perpendicular wave vector, and $\mathrm{J}_l(\lambda_k)$ is the Bessel function of order $l$.

Compared with the W matrix in Ref. 29, the most significant modification in the energy absorption is that the gyrofrequency here is space dependent. In contrast, the effects due to the gradients of the density and temperature can be neglected except for drift wave range of frequency. Thus taking $K_{\nabla} \approx 1$ and completing the velocity integration yields

$$W_l(\mathbf{k}, \mathbf{k}') = \mathbf{TE}_k{}^{\dagger}\cdot\mathbf{W}_l^{(0)}(\mathbf{k}, \mathbf{k}')\cdot\mathbf{TE}_{k'}, \tag{A11}$$

where the same Cartesian coordinate system (x, y, z) as that in Sec. IV is used, $\mathbf{TE}_k \equiv (e^{-i\theta_k}E_+, e^{i\theta_k}E_-, E_z)$, $\theta_k \equiv \arcsin(k_y/k_{\perp})$,

$$\mathbf{W}_l^{(0)} = -i\frac{\varepsilon_0\omega_p^2}{2k_z v_T}\mathrm{e}^{-\bar{\Gamma}}Z(\zeta_l)\cdot\begin{pmatrix} (1-\bar{\Gamma})I_{l-1}+\tilde{\Gamma}I'_{l-1} & (\Gamma_{k'}I_{l-1}+\Gamma_k I_{l+1})/2-\tilde{\Gamma}I_l & \zeta_l(k'_\perp I_{l-1}-k_\perp I_l)\rho \\ (\Gamma_k I_{l-1}+\Gamma_{k'}I_{l+1})/2-\tilde{\Gamma}I_l & (1-\bar{\Gamma})I_{l+1}+\tilde{\Gamma}I'_{l+1} & \zeta_l(k_\perp I_l-k'_\perp I_{l+1})\rho \\ \zeta_l(k_\perp I_{l-1}-k'_\perp I_l)\rho & \zeta_l(k'_\perp I_l-k_\perp I_{l+1})\rho & 4\zeta_l^2 I_l \end{pmatrix}, \quad \text{(A12)}$$

$\omega_p^2 \equiv nq^2/(\varepsilon_0 m)$, $\zeta_l \equiv (\omega - l\Omega)/k_z$, $\Gamma_k = (k_\perp v_T/\Omega)^2/2$, $\tilde{\Gamma} \equiv k_\perp k'_\perp k'_\perp/2$, $\bar{\Gamma} = (\Gamma_k + \Gamma_{k'})/2$, $\mathrm{I}_l' = \mathrm{d}\mathrm{I}_l(\tilde{\Gamma})/\mathrm{d}\tilde{\Gamma}$, and $\mathrm{I}_l = \mathrm{I}_l(\tilde{\Gamma})$ is the modified Bessel function of order $l$. When $\theta_k = \theta_{k'} = 0$, $W_l(\mathbf{k},\mathbf{k}')$ in Eq. (A11) reduces to $\mathbf{E}_m^* \cdot \mathbf{W}_l \cdot \mathbf{E}_n$ in Ref. 28 and is used as the resonant energy absorption which induces the collisionless damping of the model wave in Sec. IV.

## APPENDIX B: MANIPULATION FOR RF FORCES

### 1. Stresses in the guiding-center formulation

In this appendix, we summarize various stress terms in the guiding-center formulation. The electromagnetic stress is

$$\mathbf{\Pi}_{\mathrm{DE}} = \frac{q}{2\Omega}\mathrm{Re}\sum_{k,k'}\mathrm{e}^{i(\mathbf{k}'-\mathbf{k})\cdot\mathbf{r}}\int \mathrm{d}^3\mathbf{v} f_{k'}\mathbf{b}\times\mathbf{v}\left(1-\frac{\mathbf{k}'\cdot\mathbf{v}}{\omega}\right)\mathbf{E}_k^* + \frac{1}{2}\mathrm{Re}\sum_{k,k'}\mathrm{e}^{i(\mathbf{k}'-\mathbf{k})\cdot\mathbf{r}}\left(\mathbf{D}_{k',//}\mathbf{E}_{k,//}^* - \frac{in_0 q}{\omega B}\mathbf{b}\times\mathbf{E}_{k'}\mathbf{E}_{k,//}^*\right), \quad \text{(B1)}$$

where we retain the term $\mathbf{b}\times\mathbf{E}\mathbf{E}_{//}^*$ in the second bracket, which was neglected in Ref. 29 by appealing to the argument of the species summed quasineutrality. The off-diagonal pressure tensor is[29]

$$\mathbf{\Pi}_\phi = \left\langle \frac{m}{\Omega}\int \mathrm{d}^3\mathbf{v}\frac{1}{4}(\mathbf{v}_\perp\mathbf{a}\times\mathbf{b} + \mathbf{a}_\perp\mathbf{v}\times\mathbf{b})f_1\right\rangle_t + \left\langle \frac{m}{\Omega}\int \mathrm{d}^3\mathbf{v}(\mathbf{v}_{//}\mathbf{a}\times\mathbf{b} + \mathbf{a}_{//}\mathbf{v}\times\mathbf{b})f_1\right\rangle_t + tr, \quad \text{(B2)}$$

where $tr$ indicates the transpose of all the preceding terms.

The diagonal pressure tensor for the general electromagnetic wave was given in Eq. (B4) in Ref. 57 as

$$\frac{\partial}{\partial t}(\mathbf{\Pi}_{\mathrm{CGL}})_{\perp\perp} = m\int \mathrm{d}^3\mathbf{v}\langle f_1\mathbf{a}_1\cdot\mathbf{v}_\perp\mathrm{I}_\perp + 2f_1\mathbf{a}_1\cdot\mathbf{v}_{//}\mathbf{b}\mathbf{b}\rangle_t. \quad \text{(B3)}$$

### 2. Perpendicular forces due to perpendicular gradients

For the perpendicular forces due to perpendicular gradients, combining Eqs. (27), (B1), and (B2) can yield[29]

$$-[\nabla_\perp\cdot(\mathbf{\Pi}_w + \mathbf{\Pi}_{DE} + \mathbf{\Pi}_\phi)]_\perp = -\nabla_\perp X_r + \mathbf{b}\times\nabla X_d, \quad \text{(B4)}$$

where

$$X_r = \frac{m}{2\Omega}\left\langle\int \mathrm{d}^3 v\mathbf{b}\times\mathbf{v}\cdot\mathbf{a}f_1\right\rangle_t, \qquad X_d = \frac{m}{2\Omega}\left\langle\int \mathrm{d}^3 v\mathbf{v}_\perp\cdot\mathbf{a}f_1\right\rangle_t. \quad \text{(B5)}$$

Here, $X_d$ is resonant and is evaluated to be $\dot{w}_\perp/(2\Omega)$ by using the lowest-order $f_1$ in Eq. (A5), where $\dot{w}_\perp$ obtained in Ref. 29 is

$$\dot{w}_\perp = \frac{1}{2}\mathrm{Re}\sum_{k,k'}\mathrm{e}^{i(\mathbf{k}'-\mathbf{k})\cdot\mathbf{r}}\sum_l\frac{l\Omega}{2\omega}W_l(\mathbf{k},\mathbf{k}'). \quad \text{(B6)}$$

Thus, the poloidal RPF in Eq. (5) is obtained from $\mathbf{b}\times\nabla X_d$. $X_r$ can be recast as

$$X_r = \frac{1}{2}\mathrm{Re}\sum_{k,k'}\mathrm{e}^{i(\mathbf{k}'-\mathbf{k})\cdot\mathbf{r}} \times\left\{\frac{1}{2}i\frac{\mathbf{k}_\perp}{\omega}\cdot\frac{\partial}{\partial\mathbf{k}_\perp}W(\mathbf{k},\mathbf{k}') + i\frac{q}{2}\int \mathrm{d}^3\mathbf{v}\left(\frac{\mathbf{E}_{k\perp}{}^*\cdot\mathbf{v}}{\omega}\right)f_{k'}\right\} \equiv X_{r,k\perp} + X_{r,\perp}, \quad \text{(B7)}$$

where $X_{r,\perp}$ was missed in Ref. 29 but it is needed to cancel $\mathbf{\Pi}_{\mathrm{CGL},E\perp}$ given in Eq. (B8) below. The operator $\partial/\partial\mathbf{k}$ in Eq. (C12) in Ref. 29 might be mistaken with $\partial/\partial\mathbf{k}_\perp$ in Eq. (C14) there.

Substituting the lowest-order $f_1$ into Eq. (B3) and using the slowing-ramped-field correction for the time integration,[58] we obtain

$$\mathbf{\Pi}_{\mathrm{CGL},\perp\perp} = \mathrm{I}_\perp\frac{1}{2}\mathrm{Re}\sum_{k,k'}\mathrm{e}^{i(\mathbf{k}'-\mathbf{k})\cdot\mathbf{r}}t\sum_l\frac{l\Omega}{\omega}W_l + \mathrm{I}_\perp\frac{1}{2}\mathrm{Re}\sum_{k,k'}\mathrm{e}^{i(\mathbf{k}'-\mathbf{k})\cdot\mathbf{r}}\sum_l\frac{il\Omega}{2\omega}\frac{\partial W_l}{\partial\omega} - \mathrm{I}_\perp\frac{1}{2}\mathrm{Re}\sum_{k,k'}\mathrm{e}^{i(\mathbf{k}'-\mathbf{k})\cdot\mathbf{r}}\frac{iq}{2}\int \mathrm{d}^3\mathbf{v}\left(\frac{\mathbf{E}_{k\perp}{}^*\cdot\mathbf{v}}{\omega}\right)f_{k'} \equiv \mathbf{\Pi}_{\mathrm{CGL,sec}} + \mathbf{\Pi}_{\mathrm{CGL},\partial\omega} + \mathbf{\Pi}_{\mathrm{CGL},E\perp}. \quad \text{(B8)}$$

Thus, the secular radial pressure gradient, the second term in $(\mathbf{F}_\nabla)_\perp$ in Eq. (5), is obtained from $-\nabla\cdot\mathbf{\Pi}_{\mathrm{CGL,sec}}$. The second term in Eq. (B8) $\mathbf{\Pi}_{\mathrm{CGL},\partial\omega}$ may be viewed as the nonresonant pressure.

The nonresonant force $\mathbf{F}_{\mathrm{nr}}$ in Eq. (6) can be obtained by collecting all the nonresonant components in Eqs. (B7), (B8), and (26).

### 3. The parallel RPF due to perpendicular gradients

The zero-order (in $\rho/L_\perp$) $\mathbf{a}_k^*\times\mathbf{b}$ can be recast as

$$\mathbf{a}_k^*\times\mathbf{b} = \frac{q}{m}\mathbf{E}_k^*\times\mathbf{b}\left(1-\frac{\mathbf{k}'\cdot\mathbf{v}}{\omega}\right) + \frac{\mathbf{k}}{\omega}\times\mathbf{b}\left(\frac{q}{m}\mathbf{E}_k^*\cdot\mathbf{v}\right), \quad \text{(B9)}$$

where the difference between $\mathbf{k}$ and $\mathbf{k}'$ is omitted. Taking the $v_{//}$ moment of the lowest-version of the linearized Vlasov equation, we have

$$i(\omega - \mathbf{k}'\cdot\mathbf{v})v_{//}f_{k'} = \nabla_v\cdot\left(v_{//}\mathbf{v}\times\mathbf{b}\Omega f_{k'}\right) + \nabla_v\cdot\left(v_{//}\mathbf{a}_{k'}f_0\right) - (q/m)\left[E_{//k'} + (\mathbf{v}\times\mathbf{B}_{k'})_{//}\right]f_0. \quad \text{(B10)}$$

By using these two identities and noting $f_0 \approx f_M(v^2)$ to the lowest order in $\rho/L_\perp$, the first term at the RHS of Eq. (30) becomes

$$-\nabla_\perp\cdot\left\langle\frac{m}{\Omega}\int d^3\mathbf{v}(\mathbf{a}_1\times\mathbf{b}v_{//})f_1\right\rangle_t = -\frac{1}{2}\mathrm{Re}\nabla_\perp\cdot\sum_{k,k'}e^{i(\mathbf{k}'-\mathbf{k})\cdot\mathbf{r}}\frac{in_0q}{\omega B}\mathbf{b}\times\mathbf{E}_{k'}E^*_{k//},$$
$$-\nabla_\perp\cdot\frac{q}{2\Omega}\mathrm{Re}\sum_{k,k'}e^{i(\mathbf{k}'-\mathbf{k})\cdot\mathbf{r}}\int d^3\mathbf{v}\frac{\mathbf{k}}{\omega}\times\mathbf{b}(\mathbf{E}^*_k\cdot\mathbf{v})v_{//}f_{k'}. \quad \text{(B11)}$$

The first term at the RHS of Eq. (B11) just cancels the second term at the RHS of Eq. (30). The expression of the second term at the RHS of Eq. (B11) is similar to $\langle\mathbf{J}_1\cdot\mathbf{E}_1\rangle_t$ except an additional factor $v_{//}$. Noting that this term is a symmetric bilinear form on $\mathbf{E}_k$ (or $\mathbf{E}_{k'}$) to the lowest order in $\rho/L_\perp$ and thus is totally resonant, we can set $v_{//}$ as $v_l^{(\mathrm{res})} = (\omega - l\Omega)/k_{//}$ to obtain the final result in Eq. (31).

## APPENDIX C: MOMENTUM CONSERVATION FOR A MONOCHROMATIC WAVE

The MCE for a monochromatic wave propagating in homogeneous plasma can be obtained by the similar approach as that for the energy conservation equation (ECE) (aka Poynting's theorem for plasma waves). The approach for the ECE is, in principle, recasting the linear current by the dot product of the conductivity and the electric field in Fourier representation and substituting it to the general Poynting's theorem for EM waves.[59] The general MCE for EM waves is

$$\frac{\partial}{\partial t}(\varepsilon_0\mathbf{E}_1\times\mathbf{B}_1) + \nabla\cdot\left[\left(\varepsilon_0|E_1|^2 + \frac{1}{\mu_0}|B_1|^2\right)\mathbf{I} - \varepsilon_0\mathbf{E}_1\mathbf{E}_1 - \frac{1}{\mu_0}\mathbf{B}_1\mathbf{B}_1\right] = -\mathbf{F}_{\mathrm{EM}}, \quad \text{(C1)}$$

which is obtained by using Maxwell's equations to replace the linear current in the definition of the EM force

$$\mathbf{F}_{\mathrm{EM}} = \sum_j(n_{j,1}q_j\mathbf{E}_1 + \mathbf{J}_{j,1}\times\mathbf{B}_1), \quad \text{(C2)}$$

where the index $j$ indicates the species number.

Assuming the envelope of rf fields slowly varying in space and time, i.e.,

$$\mathbf{E}_1(\mathbf{r},t) = \frac{1}{2}\left[\mathbf{E}_s(\mathbf{r},t)e^{i\mathbf{k}_0\cdot\mathbf{r}-i\omega_0t} + c.c.\right], \quad \text{(C3)}$$

recasting $\mathbf{J}_{j,1}$ in Fourier representation as

$$\mathbf{J}_{j,k} = \boldsymbol{\sigma}_j(\mathbf{k},\omega)\cdot\mathbf{E}_s(\mathbf{r},t) - i\frac{\partial\boldsymbol{\sigma}}{\partial\mathbf{k}}\cdot\frac{\partial\mathbf{E}_s}{\partial\mathbf{r}} + i\frac{\partial\boldsymbol{\sigma}}{\partial\omega}\cdot\frac{\partial\mathbf{E}_s}{\partial t} \quad \text{(C4)}$$

and using the linearized continuity equation to cancel $n_{j,1}$, the EM force becomes

$$\mathbf{F}_{\mathrm{EM}} = \frac{1}{2}\mathrm{Re}\left\{\frac{\mathbf{k}}{\omega}\mathbf{E}^*\cdot\boldsymbol{\sigma}\cdot\mathbf{E} + \nabla\cdot\left[\mathbf{I}\left(\mathbf{E}^*\cdot\frac{i\boldsymbol{\sigma}}{2\omega}\cdot\mathbf{E}\right) - \frac{\partial}{\partial\mathbf{k}}\left(\mathbf{E}^*\cdot\frac{i\boldsymbol{\sigma}}{2\omega}\cdot\mathbf{E}\right)\mathbf{k} - \frac{i\boldsymbol{\sigma}}{\omega}\cdot\mathbf{E}\mathbf{E}^*\right] + \frac{\partial}{\partial t}\left[\frac{\mathbf{k}}{\omega}\left(\mathbf{E}^*\cdot\frac{i\boldsymbol{\sigma}}{2\omega}\cdot\mathbf{E}\right) + \frac{\partial}{\partial\omega}\left(\mathbf{E}^*\cdot\frac{i\boldsymbol{\sigma}}{2}\cdot\mathbf{E}\right)\frac{\mathbf{k}}{\omega} - \frac{\mathbf{k}}{\omega}\cdot\frac{i\boldsymbol{\sigma}}{\omega}\cdot\mathbf{E}\mathbf{E}^*\right]\right\}, \quad \text{(C5)}$$

where $\boldsymbol{\sigma}\equiv\sum_j\boldsymbol{\sigma}_j$ and the subscript $s$ is suppressed. Then, the whole MCE can be obtained by substituting $\mathbf{F}_{\mathrm{EM}}$ into Eq. (C1). Introducing the action density $J_A$ and the action flux density $\boldsymbol{\Gamma}_A$ as follows,

$$J_A \equiv \frac{\varepsilon_0}{2}\mathbf{E}^*\cdot\frac{\partial\mathbf{M}^h}{\partial\omega}\cdot\mathbf{E}, \quad \text{(C6)}$$

$$\boldsymbol{\Gamma}_A = -\frac{\partial}{\partial\mathbf{k}}\left(\mathbf{E}^*\cdot\frac{\varepsilon_0}{2}\mathbf{M}\cdot\mathbf{E}\right), \quad \text{(C7)}$$

then the whole MCE is recast into a compact expression consistent with the wave kinetic equation as

$$\frac{\partial}{\partial t}(\mathbf{k}J_A) + \nabla\cdot(\boldsymbol{\Gamma}_A\mathbf{k}) = -\mathbf{k}\mathbf{E}^*\cdot\boldsymbol{\varepsilon}^a\cdot\mathbf{E}, \quad \text{(C8)}$$

where $\mathbf{M}\equiv(\mathbf{k}\mathbf{k} - k^2\mathbf{I})/k_0^2 + \boldsymbol{\varepsilon}/\varepsilon_0$, $\mathbf{M}^h\equiv(\mathbf{M}+\mathbf{M}^\dagger)/2$, $\boldsymbol{\varepsilon}\equiv\varepsilon_0\mathbf{I} + i\boldsymbol{\sigma}/\omega$, $\boldsymbol{\varepsilon}^a\equiv(\boldsymbol{\varepsilon}-\boldsymbol{\varepsilon}^\dagger)/2i$, and the Fourier representation of the Helmholtz equation, $\mathbf{M}\cdot\mathbf{E} = 0$, is used.

The nonresonant ponderomotive force $\mathbf{F}_{\mathrm{nr}}$ in Eq. (6) is quite different from these expressions for the change of wave momentum. The root cause is that the nonlinear kinetic stress $\boldsymbol{\Pi}_2$ is neglected in the MCE.

[1]Y. Q. Liu, A. Bondeson, Y. Gribov, and A. Polevoi, Nucl. Fusion **44**, 232 (2004).
[2]P. Politzer, C. Petty, R. Jayakumar, T. Luce, M. Wade, J. DeBoo, J. Ferron, P. Gohil, C. Holcomb, and A. Hyatt, Nucl. Fusion **48**, 075001 (2008).
[3]P. W. Terry, Rev. Mod. Phys. **72**, 109 (2000).
[4]L. G. Eriksson, T. Johnson, T. Hellsten, C. Giroud, V. G. Kiptily, K. Kirov, J. Brzozowski, M. DeBaar, J. DeGrassie, M. Mantsinen, A. Meigs, J. M. Noterdaeme, A. Staebler, D. Testa, A. Tuccillo, and K. D. Zastrow, Phys. Rev. Lett. **92**, 235001 (2004).

[5]Y. Lin, J. E. Rice, S. J. Wukitch, M. J. Greenwald, A. E. Hubbard, A. Ince-Cushman, L. Lin, M. Porkolab, M. L. Reinke, and N. Tsujii, Phys. Rev. Lett. **101**, 235002 (2008).
[6]L. G. Eriksson, T. Hellsten, M. F. F. Nave, J. Brzozowski, K. Holmstrom, T. Johnson, J. Ongena, K. D. Zastrow, and J.-E. Contributors, Plasma Phys. Controlled Fusion **51**, 044008 (2009).
[7]A. Ince-Cushman, J. E. Rice, M. Reinke, M. Greenwald, G. Wallace, R. Parker, C. Fiore, J. W. Hughes, P. Bonoli, S. Shiraiwa, A. Hubbard, S. Wolfe, I. H. Hutchinson, E. Marmar, M. Bitter, J. Wilson, and K. Hill, Phys. Rev. Lett. **102**, 035002 (2009).
[8]Y. Lin, P. Mantica, T. Hellsten, V. Kiptily, E. Lerche, M. F. F. Nave, J. E. Rice, D. Van Eester, P. C. de Vries, R. Felton, C. Giroud, T. Tala, and J. E. Contributors, Plasma Phys. Controlled Fusion **54**, 074001 (2012).
[9]W. Y. Zhang, Y. D. Li, X. J. Zhang, T. Lan, X. Gao, Z. X. Liu, P. J. Sun, X. D. Zhang, J. Li, and HT-7 Teams, Plasma Phys. Controlled Fusion **54**, 035005 (2012).
[10]X. J. Zhang, Y. P. Zhao, B. N. Wan, X. Z. Gong, Y. Lin, W. Y. Zhang, Y. Z. Mao, C. M. Qin, S. Yuan, X. Deng, L. Wang, S. Q. Ju, Y. Chen, Y. D. Li, J. G. Li, J. M. Noterdaeme, and S. J. Wukitch, Nucl. Fusion **52**, 082003 (2012).
[11]J. S. deGrassie, K. H. Burrell, L. R. Baylor, W. Houlberg, and J. Lohr, Phys. Plasmas **11**, 4323 (2004).
[12]Y. Sakamoto, S. Ide, M. Yoshida, Y. Koide, T. Fujita, H. Takenaga, and Y. Kamada, Plasma Phys. Controlled Fusion **48**, A63 (2006).
[13]J. E. Rice, W. D. Lee, E. S. Marmar, P. T. Bonoli, R. S. Granetz, M. J. Greenwald, A. E. Hubbard, I. H. Hutchinson, J. H. Irby, Y. Lin, D. Mossessian, J. A. Snipes, S. M. Wolfe, and S. J. Wukitch, Nucl. Fusion **44**, 379 (2004).
[14]R. M. McDermott, C. Angioni, R. Dux, A. Gude, T. Putterich, F. Ryter, G. Tardini, and A. U. Team, Plasma Phys. Controlled Fusion **53**, 035007 (2011).
[15]Y. J. Shi, G. S. Xu, F. D. Wang, M. Wang, J. Fu, Y. Y. Li, W. Zhang, W. Zhang, J. F. Chang, B. Lv, J. P. Qian, J. F. Shan, F. K. Liu, S. Y. Ding, B. N. Wan, and S. G. Lee, Phys Rev Lett **106**, 235001 (2011).
[16]M. F. F. Nave, L. G. Eriksson, C. Giroud, T. J. Johnson, K. Kirov, M. L. Mayoral, J. M. Noterdaeme, J. Ongena, G. Saibene, R. Sartori, F. Rimini, T. Tala, P. de Vries, K. D. Zastrow, and J.-E. Contributors, Plasma Phys. Controlled Fusion **54**, 074006 (2012).
[17]J. E. Rice, Y. A. Podpaly, M. L. Reinke, C. Gao, S. Shiraiwa, J. L. Terry, C. Theiler, G. M. Wallace, P. T. Bonoli, D. Brunner, R. M. Churchill, I. Cziegler, L. Delgado-Aparicio, P. H. Diamond, I. C. Faust, N. J. Fisch, R. S. Granetz, M. J. Greenwald, A. E. Hubbard, J. W. Hughes, I. H. Hutchinson, J. H. Irby, J. Lee, Y. Lin, E. S. Marmar, R. Mumgaard, R. R. Parker, S. D. Scott, J. R. Walk, S. M. Wolfe, and S. J. Wukitch, Nucl. Fusion **53**, 093015 (2013).
[18]Y. J. Shi, W. H. Ko, J. M. Kwon, P. H. Diamond, S. G. Lee, S. H. Ko, L. Wang, S. Yi, K. Ida, L. Terzolo, S. W. Yoon, K. D. Lee, J. H. Lee, U. N. Nam, Y. S. Bae, Y. K. Oh, J. G. Kwak, M. Bitter, K. Hill, O. D. Gurcan, and T. S. Hahm, Nucl. Fusion **53**, 113031 (2013).
[19]E. F. Jaeger, L. A. Berry, J. R. Myra, D. B. Batchelor, E. D'Azevedo, P. T. Bonoli, C. K. Phillips, D. N. Smithe, D. A. D'Ippolito, M. D. Carter, R. J. Dumont, J. C. Wright, and R. W. Harvey, Phys. Rev. Lett. **90**, 195001 (2003).
[20]S. Wang, Phys. Plasmas **18**, 102502 (2011).
[21]X. Guan, H. Qin, J. Liu, and N. J. Fisch, Phys. Plasmas **20**, 022502 (2013).
[22]J. R. Myra, D. A. D'Ippolito, D. A. Russell, L. A. Berry, E. F. Jaeger, and M. D. Carter, Nucl. Fusion **46**, S455 (2006).
[23]Z. Gao, J. Chen, and N. J. Fisch, Phys. Rev. Lett. **110**, 235004 (2013).
[24]G. G. Craddock and P. H. Diamond, Phys. Rev. Lett. **67**, 1535 (1991).
[25]G. G. Craddock, P. H. Diamond, M. Ono, and H. Biglari, Phys. Plasmas **1**, 1944 (1994).
[26]L. A. Berry, E. F. Jaeger, and D. B. Batchelor, Phys. Rev. Lett. **82**, 1871 (1999).
[27]E. F. Jaeger, L. A. Berry, and D. B. Batchelor, Phys. Plasmas **7**, 641 (2000).
[28]E. F. Jaeger, L. A. Berry, and D. B. Batchelor, Phys. Plasmas **7**, 3319 (2000).
[29]J. R. Myra, L. A. Berry, D. A. D'Ippolito, and E. F. Jaeger, Phys. Plasmas **11**, 1786 (2004).
[30]V. Chan and S. Chiu, Phys. Fluids B **5**, 3590 (1993).
[31]A. Fukuyama, K. Itoh, S. I. Itoh, and K. Hamamatsu, Phys. Fluids B **5**, 539 (1993).
[32]J. R. Myra and D. A. D'Ippolito, Phys. Plasmas **9**, 3867 (2002).
[33]Z. Gao, N. J. Fisch, and H. Qin, Phys. Plasmas **13**, 112307 (2006).
[34]$l = 0$ corresponds to Landau damping, which is also included.
[35]Z. Gao, N. J. Fisch, H. Qin, and J. R. Myra, Phys. Plasmas **14**, 084502 (2007).
[36]J. Chen, Ph.D. dissertation, Chinese Academy of Sciences, 2013 (in Chinese).
[37]L. A. Berry and E. F. Jaeger, AIP Conf. Proc. **595**, 426 (2001).
[38]The second-order rf kinetic theory can obtain the collisionless flux more conveniently than the guiding-center formulation.
[39]J. R. Myra, D. A. D'Ippolito, L. A. Berry, E. F. Jaeger, and D. B. Batchelor, AIP Conf. Proc. **694**, 487 (2003).
[40]T. Hellsten, Plasma Phys. Controlled Fusion **53**, 054007 (2011).
[41]C. Lashmore-Davies and R. Dendy, Phys. Fluids B **4**, 493 (1992).
[42]C. N. Lashmore-Davies and R. O. Dendy, Phys. Fluids **1**, 1565 (1989).
[43]E. F. Jaeger, private communication (2012).
[44]P. T. Bonoli and R. C. Englade, Phys. Fluids **29**, 2937 (1986).
[45]P. T. Bonoli and E. Ott, Phys. Rev. Lett. **46**, 424 (1981).
[46]R. Cesario, A. Cardinali, C. Castaldo, F. Paoletti, W. Fundamenski, S. Hacquin, and JET-EFDA Workprogramme Contributors, Nucl. Fusion **46**, 462 (2006).
[47]C. S. Liu and V. K. Tripathi, Phys. Rep. **130**, 143 (1986).
[48]J. R. Martin-Solis, R. Sanchez, and B. Esposito, Phys. Plasmas **9**, 1667 (2002).
[49]J. M. Rax, L. Laurent, and D. Moreau, Europhys. Lett. **15**, 497 (1991).
[50]E. J. Valeo and N. J. Fisch, Phys. Rev. Lett. **73**, 3536 (1994).
[51]Y. Lin, J. E. Rice, S. J. Wukitch, M. J. Greenwald, A. E. Hubbard, A. Ince-Cushman, L. Lin, E. S. Marmar, M. Porkolab, M. L. Reinke, N. Tsujii, J. C. Wright, and A. C.-M. Team, Phys. Plasmas **16**, 056102 (2009).
[52]M. Brambilla, Plasma Phys. Controlled Fusion **41**, 1 (1999).
[53]M. Yoshida, S. Kaye, J. Rice, W. Solomon, T. Tala, R. E. Bell, K. H. Burrell, J. Ferreira, Y. Kamada, D. McDonald, P. Mantica, Y. Podpaly, M. L. Reinke, Y. Sakamoto, A. Salmi, and I. T. C. Topical, Nucl. Fusion **52**, 123005 (2012).
[54]D. N. Smithe, Plasma Phys. Controlled Fusion **31**, 1105 (1989).
[55]We apply for $f_1$ the convectional Fourier representation on the particle position space here instead of that on the guiding-center space in the original work by Myra *et al*.
[56]L. Chen and S-T. Tsai, Plasma Phys. **25**, 349 (1983).
[57]J. R. Myra and D. A. D'lppolito, Phys. Plasmas **7**, 3600 (2000).
[58]J. Chen and Z. Gao, Phys. Plasmas **20**, 082508 (2013).
[59]T. H. Stix, *Waves in Plasmas* (Springer, New York, 1992), p. 74.